

## Stability of amorphous Se/Se $100-x$ Te $x$ multilayers: A Raman study

D. Nesheva, I. P. Kotsalas, C. Raptis, and D. Arsova

Citation: *Journal of Applied Physics* **86**, 4964 (1999); doi: 10.1063/1.371467

View online: <http://dx.doi.org/10.1063/1.371467>

View Table of Contents: <http://scitation.aip.org/content/aip/journal/jap/86/9?ver=pdfcov>

Published by the [AIP Publishing](#)

---

### Articles you may be interested in

[Reversible amorphous-crystalline phase changes in a wide range of Se \$\_{1-x}\$ Te \$\_x\$  alloys studied using ultrafast differential scanning calorimetry](#)

*J. Chem. Phys.* **141**, 024502 (2014); 10.1063/1.4886185

[Photoluminescence properties and crystallization of silicon quantum dots in hydrogenated amorphous Si-rich silicon carbide films](#)

*J. Appl. Phys.* **115**, 164303 (2014); 10.1063/1.4871980

[Laser-induced suppression of photocrystallization rate in amorphous selenium films](#)

*J. Appl. Phys.* **83**, 4951 (1998); 10.1063/1.367296

[Short-pulse laser-induced crystallization of intrinsic and hydrogenated amorphous germanium thin films](#)

*J. Appl. Phys.* **82**, 5159 (1997); 10.1063/1.366320

[Laser crystallization and structuring of amorphous germanium](#)

*Appl. Phys. Lett.* **70**, 3570 (1997); 10.1063/1.119236

---



Launching in 2016!  
The future of applied photonics research is here

**AIP** | APL  
Photonics

# Stability of amorphous Se/Se<sub>100-x</sub>Te<sub>x</sub> multilayers: A Raman study

D. Nesheva,<sup>a)</sup> I. P. Kotsalas, and C. Raptis<sup>b)</sup>

*Physics Department, National Technical University of Athens, GR-15780 Athens, Greece*

D. Arsova

*Institute of Solid State Physics, Bulgarian Academy of Sciences, 1784 Sofia, Bulgaria*

(Received 14 April 1999; accepted for publication 30 July 1999)

The Raman spectra of amorphous Se/Se<sub>100-x</sub>Te<sub>x</sub> multilayers (AMLs) of various compositions and sublayer thicknesses have been measured at room and low temperature (38 K) with the aim to assess the thermal and absorption effects of laser illumination on the structural stability of the AMLs. Under thermal treatment at room temperature (mediated by increasing gradually the power of the probing laser line), the AML stability (manifested by the rate of Se crystallization) increases with decreasing Se<sub>100-x</sub>Te<sub>x</sub> sublayer thickness and with decreasing Te content. However, in single layers (2  $\mu\text{m}$  thickness) of Se<sub>100-x</sub>Te<sub>x</sub>, we have observed the opposite effect, that is, the stability of single layers increases with increasing Te content. This apparent contradiction is explained in terms of thermodynamic energy considerations stated previously [K. Tanaka *et al.*, Mater. Res. Soc. Symp. Proc. **118**, 343 (1988)] and of a higher crystallization temperature of Se sublayers in the AMLs than that of bulk Se of the single layer. In order to eliminate (or, at least, reduce considerably) the thermal effects of laser illumination and study the photoinduced structural changes (due to absorption) in Se/Se<sub>100-x</sub>Te<sub>x</sub> AMLs, low temperature (38 K) measurements were carried out using the 530.9 nm Kr<sup>+</sup> laser line which is strongly absorbed by these AMLs. The rate of photoinduced crystallization increases with increasing Te content, which means that their stability to photoinduced changes is (again) higher, the lower the Te content. This is in agreement with previous results concerning three-dimensional Se<sub>100-x</sub>Te<sub>x</sub> alloys, implying that the dimensionality change (from 3 in the alloys to 2 in the AMLs) does not affect significantly the Se–Se and Se–Te bond energies. © 1999 American Institute of Physics. [S0021-8979(99)05821-1]

## I. INTRODUCTION

Amorphous selenium (*a*-Se) is a widely used material in conventional photocopying machines<sup>1</sup> and experimental vidicon pickup tubes.<sup>2</sup> However, its low crystallization temperature and low photosensitivity in the yellow-red region of the spectrum are often serious drawbacks for such applications. In order to extend the region of photosensitivity and increase the crystallization temperature, tellurium doping has been used,<sup>1</sup> but when the tellurium concentration is higher than 10 at. % (a doping rate necessary for laser printer applications), there are counter-productive effects involving a reduction of the charge acceptance, a faster dark charge decay and an increase of the residual voltage.<sup>1</sup> These effects are due to a strong increase of the density of shallow and deep traps leading to a serious drop of the electron and hole drift mobilities.<sup>3,4</sup> It has been pointed out<sup>1,2</sup> that the only practical solution to avoid these undesired effects in Se–Te alloys with relatively high Te content is to design multilayer photoreceptor structures with separate layers for photogeneration and for charge transport.<sup>1,2</sup>

Photoreceptors with an amorphous multilayer (AML) structure of Se/Se<sub>100-x</sub>Te<sub>x</sub> acting as the photogeneration layer, have demonstrated<sup>5,6</sup> high photosensitivity in the red

and near-infrared regions, as well as a slow dark charge decay and a good contrast. The photosensitivity and thermal stability of photoreceptors comprising Se/Se<sub>100-x</sub>Te<sub>x</sub> AMLs depends on their sublayer thickness, interface quality and Te content. Since these AMLs are built of sublayers of similar materials, x-ray diffraction cannot be used for studying their structural features. The observed step-wise behavior in their absorption spectra<sup>7</sup> and the bumps in the current–voltage characteristics of the conductivity in a direction perpendicular to the layer planes<sup>8</sup> of Se/Se<sub>85</sub>Te<sub>15</sub> AML (deposited by the laser ablation technique) could be considered as indirect pieces of evidence for high quality AMLs.

In this article, Raman scattering measurements have been carried out on Se/Se<sub>100-x</sub>Te<sub>x</sub> AMLs of various Te content and sublayer thicknesses (2.7–10 nm) and the attention is focused on the stability of these AMLs under various thermal and light treatments. Raman scattering is a unique probing technique for the study of such low-dimensional amorphous multilayers, not only for the structural characterization of the layers, but also for the detection of even marginal structural changes under various treatments, which cannot be resolved by x-ray diffraction techniques.

## II. EXPERIMENT

Amorphous multilayers of Se/Se<sub>100-x</sub>Te<sub>x</sub> were prepared by alternative thermal evaporation (deposition rate  $V_d = 0.5$  nm/s) of previously synthesized and powdered glassy Se and

<sup>a)</sup>Permanent address: Institute of Solid State Physics, Bulgarian Academy of Sciences, 1784 Sofia, Bulgaria.

<sup>b)</sup>Electronic mail: craptis@central.ntua.gr

$\text{Se}_{100-x}\text{Te}_x$  ( $x=7.5, 15, 30$ ) from two independent tantalum crucibles. Corning 7059 glass substrates at room temperature were used for the deposition. All details concerning the multilayer preparation procedures have been described elsewhere.<sup>6,9</sup> Here, we note that the  $x$  values for Te content quoted above correspond to the source material. In  $\text{Se}_{100-x}\text{Te}_x$  sublayers of AMLs, the Te content should be lower by up to 20% compared to the source material and this is concluded by analogy to the Te content reduction measured (using the Ague technique) in the case of  $\text{Se}_{100-x}\text{Te}_x$  single layers prepared by evaporation of the respective glass. As has been shown previously,<sup>1,6</sup> the Te content in  $\text{Se}_{100-x}\text{Te}_x$  films increases close to the layer top. A similar Te increase may be expected in the top layers of  $\text{Se}_{100-x}\text{Te}_x$  in Se/Se-Te AMLs. In order to minimize this effect, a large quantity of the respective  $\text{Se}_{100-x}\text{Te}_x$  powder was loaded in the crucible so that no more than half of it evaporated during the AML preparation.

In order to study the effect of both the sublayer thickness and Te content on the thermal and photoinduced crystallization of  $\text{Se}_{100-x}\text{Te}_x$  sublayers of Se/Se-Te AMLs, two groups of samples were produced: (i) AMLs of Se/ $\text{Se}_{70}\text{Te}_{30}$  having five different thicknesses of the  $\text{Se}_{70}\text{Te}_{30}$  sublayers ( $d_w = 2.7, 3.5, 5.0, 7.0$ , and  $10$  nm) and (ii) AMLs of Se/ $\text{Se}_{100-x}\text{Te}_x$  of various  $x$  (7.5, 15, and 30), but of the same thickness (7 nm) for the  $\text{Se}_{100-x}\text{Te}_x$  sublayers. The total thickness of the various AMLs was between 160 and 190 nm.

As was mentioned above, the introduction of Te to Se increases its glass transition and crystallization temperatures. This means that the crystallization temperature of  $\text{Se}_{100-x}\text{Te}_x$  sublayers in Se/ $\text{Se}_{100-x}\text{Te}_x$  AMLs may be higher than that of Se sublayers. On the other hand, it has been established previously<sup>10</sup> that the crystallization temperature  $T_c$  of Se in Se/CdSe AMLs increases strongly with decreasing sublayer thickness. Therefore, in order to ensure a high  $T_c$  of Se in Se/ $\text{Se}_{70}\text{Te}_{30}$  AMLs, all AMLs have been prepared with a fixed Se sublayer thickness of as small as 4.0 nm. Moreover, the effect of thickness on the crystallization temperature of  $\text{Se}_{70}\text{Te}_{30}$  sublayers has been explored by exposing the samples to the 647.1 nm  $\text{Kr}^+$  laser line which is strongly absorbed ( $\alpha > 10^5 \text{ cm}^{-1}$ ) by  $\text{Se}_{70}\text{Te}_{30}$  sublayers,<sup>11</sup> but weakly so by Se<sup>12</sup> ( $\alpha \approx 5 \times 10^3 \text{ cm}^{-1}$ ).

Raman spectra of fresh and annealed AMLs of Se/ $\text{Se}_{100-x}\text{Te}_x$  were measured using a system of a SPEX double monochromator and cooled photomultiplier in conjunction with photon counting equipment. The 647.1 and 530.9 nm lines of a  $\text{Kr}^+$  laser were used for the excitation, while the spectral resolution was  $\sim 3.5 \text{ cm}^{-1}$ . The laser beam was focused on the sample surface by a cylindrical lens and its power density was varied between 8 and  $135 \text{ W/cm}^2$ . Most Raman spectra were measured at 293 K in air. The experiments concerning the photoinduced structural changes were carried out at 38 K under a vacuum of  $10^{-3}$  Pa. Some samples were annealed for two hours at  $T=325$  K in air. After normalization according to the Bose-Einstein thermal factor and noise subtraction (as a baseline), the spectra were deconvoluted by fitting the peaks to Gaussian functions and

the position and integrated intensity of the bands were determined.

### III. RESULTS AND DISCUSSION

#### A. Thermal stability

##### 1. Effect of sublayer thickness

Since a measure of the thermal stability of amorphous materials is their crystallization temperature  $T_c$  and in order to study the effect of layer thickness on the stability of  $\text{Se}_{70}\text{Te}_{30}$  sublayers in Se/ $\text{Se}_{70}\text{Te}_{30}$  AMLs, a sequence of Raman spectra were recorded from different (neighboring) spots of each sample at room temperature by increasing gradually the laser (647.1 nm  $\text{Kr}^+$  laser line) power density from 17 to  $120 \text{ W/cm}^2$ . Raman spectra of Se/ $\text{Se}_{70}\text{Te}_{30}$  AMLs having  $\text{Se}_{70}\text{Te}_{30}$  sublayer thickness of 10, 5, 3.5, and 2.7 nm are shown in Figs. 1(a)–1(d), respectively. It should be pointed out that in this series of measurements the laser beam acted simultaneously as the exciting (probing) radiation for the Raman spectra as well as the source for illumination of the samples. Specifically, for a given sample, the various spectra correspond to *different* power densities and spots, but to *identical* exposure times (to the laser beam) of 30 min, which is the time required for scanning each spectrum (recording time). It has been found that when the exposure time is increased (above 30 min) by either reducing the scanning speed or subjecting the samples to preliminary illumination (see Sec. III B), the extent of crystallization increases.

Two main bands appear in all spectra [Figs. 1(a)–1(d)] when excited with the lowest power density of  $17 \text{ W/cm}^2$ . The band at  $252 \text{ cm}^{-1}$  is due to Se-Te vibrations in  $\alpha\text{-Se}$ ,<sup>10,13–15</sup> and is accompanied by a shoulder at about  $235 \text{ cm}^{-1}$ . In Se/ $\text{Se}_{100-x}\text{Te}_x$  AMLs, there should be contributions to this band from both types of sublayers. The other band at about  $217 \text{ cm}^{-1}$  has been attributed to the vibrations of Se-Te bonds.<sup>16</sup> This assignment is confirmed by the results of this work as the intensity of this band increases with increasing  $\text{Se}_{70}\text{Te}_{30}$  sublayer thickness (which corresponds to an increasing average Te content in AMLs), almost up to a level equal to that of the  $252 \text{ cm}^{-1}$  band.

One can see from Fig. 1 that the band at  $217 \text{ cm}^{-1}$  shifts to lower frequencies when the power density is increased. It is known<sup>17</sup> that, due to interchain interactions in trigonal crystalline Se and Te, the main Raman bands (at 237 and  $122 \text{ cm}^{-1}$ , respectively) are redshifted with respect to the characteristic bands of  $\alpha\text{-Se}$  and  $\alpha\text{-Te}$  (252 and  $\sim 150 \text{ cm}^{-1}$ ). By analogy with atomic Se and Te, we relate the observed redshift of the band at  $217 \text{ cm}^{-1}$  to interchain interactions in crystallized  $\text{Se}_{70}\text{Te}_{30}$  sublayers. This redshift may be considered as an indication that crystallization occurs first in  $\text{Se}_{70}\text{Te}_{30}$  sublayers, rather than in Se ones. This consideration is consistent with the low absorption coefficient<sup>12</sup> of Se at  $\lambda=647.1$  nm. It can also be seen from Fig. 1 that the intensity of the shoulder at about  $235 \text{ cm}^{-1}$  increases with increasing laser power for all AMLs of this series. On the other hand, the band at  $252 \text{ cm}^{-1}$  decreases considerably in the spectra of AMLs with  $\text{Se}_{70}\text{Te}_{30}$  sublayer thicknesses of 10 and 5 nm [Figs. 1(a) and 1(b)] but it is not affected in the

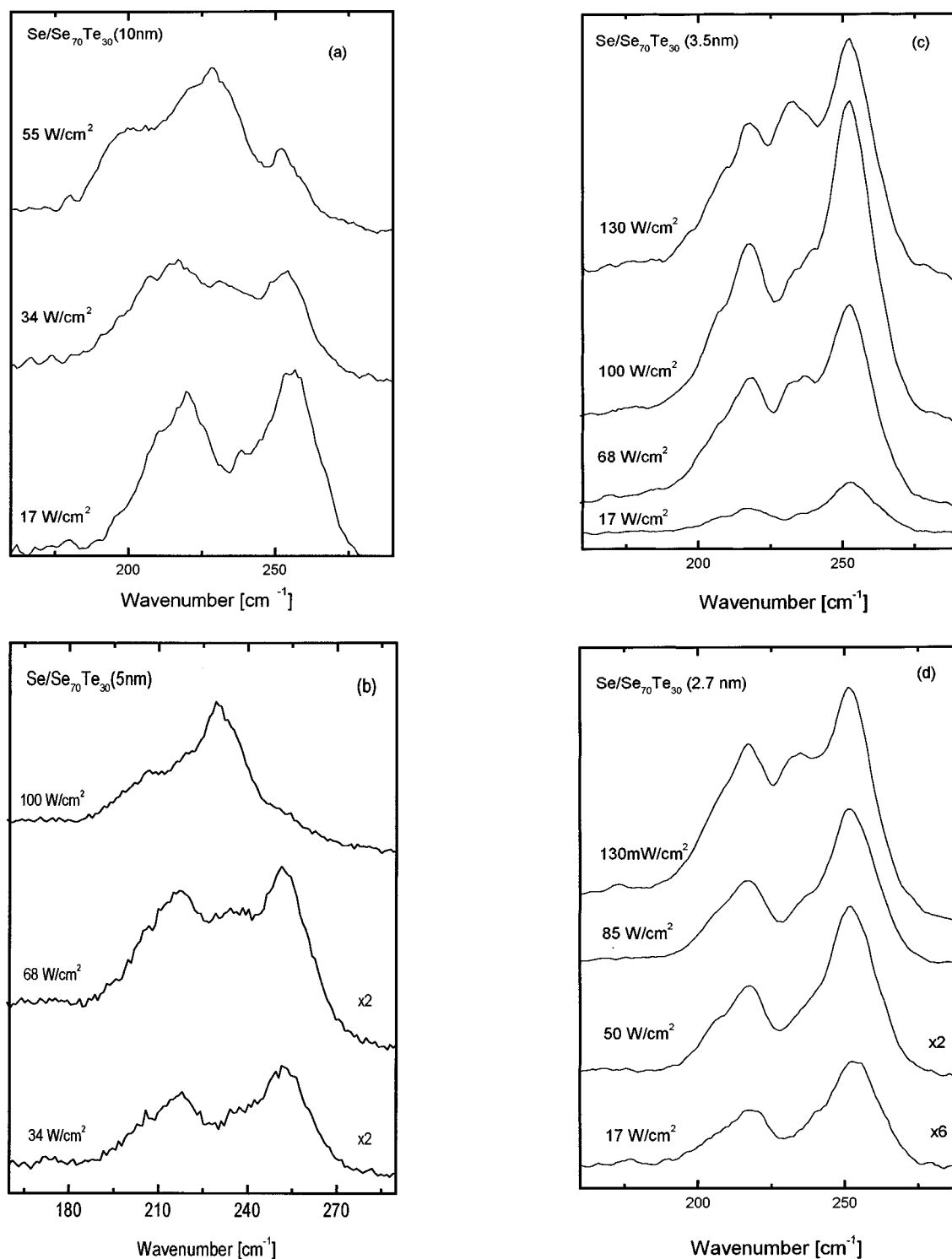


FIG. 1. Room temperature Raman spectra of Se/Se<sub>70</sub>Te<sub>30</sub> AMLs with Se<sub>70</sub>Te<sub>30</sub> sublayer thickness of (a) 10, (b) 5, (c) 3.5, and (d) 2.7 nm excited by various power densities of the 647.1 nm Kr<sup>+</sup> laser line. Each spectrum corresponds to different spot of the respective sample, but to an identical exposure time of 30 min which is equal to the recording time of the spectra.

spectra corresponding to Se<sub>70</sub>Te<sub>30</sub> sublayer thicknesses of 3.5 and 2.7 nm [Figs. 1(c) and 1(d)]. As was mentioned above, the band at 235 cm<sup>-1</sup> is related<sup>13</sup> to Se–Se bond vibrations in trigonal Se. Assuming that crystallization in Se sublayers follows that in Se<sub>70</sub>Te<sub>30</sub> ones, we use the intensity of this band as a measure of the thermal stability of the Se<sub>70</sub>Te<sub>30</sub> sublayers under exposure to the 647.1 nm laser line at room

temperature. It has been shown that crystallization in Se single layers,<sup>14,18</sup> or in the Se sublayers of Se/CdSe AMLs<sup>10</sup> is primarily a thermal process owing to the laser heating. Most likely, local heating in the Se<sub>70</sub>Te<sub>30</sub> sublayers is the main reason for crystallization observed in all Se/Se<sub>70</sub>Te<sub>30</sub> AMLs when exposed to laser light at room temperature.

Comparing the Raman spectra shown in Fig. 1, one can



see a strong increase in intensity of the  $235\text{ cm}^{-1}$  band in the AMLs having  $d_w = 10$  and  $5\text{ nm}$  when these samples are illuminated with a power density of  $50$  and  $100\text{ W/cm}^2$ , respectively. In AMLs having thinner sublayers, this increase is not so strong, even when they are exposed to a power density of  $130\text{ W/cm}^2$ . Then, assuming the intensity of the  $235\text{ cm}^{-1}$  band as a quantity of reference for the extent of crystallization in  $\text{Se/Se}_{70}\text{Te}_{30}$  AMLs, we conclude that the crystallization temperature of  $\text{Se}_{70}\text{Te}_{30}$  sublayers increases with decreasing their thickness. Such  $T_c$  increases have already been reported for the  $a\text{-Ge}$  sublayers in AMLs of  $a\text{-Ge:H/a-GeN}$ ,<sup>19</sup>  $a\text{-Si:H/a-Ge:H}$ <sup>20</sup> as well as for the  $a\text{-Se}$  sublayers in AMLs of  $a\text{-Se/CdSe}$ <sup>10</sup> and  $a\text{-Se/As}_2\text{S}_3$ .<sup>21</sup> This  $T_c$  increase with decreasing  $\text{Se}_{70}\text{Te}_{30}$  sublayer thickness is quite important for practical applications of  $\text{Se/Se}_{70}\text{Te}_{30}$  AMLs. It has already been shown<sup>6</sup> that multilayer xerographic photoreceptors, having a combination of very thin single layer of  $\text{Se}_{70}\text{Te}_{30}$  and  $\text{Se/Se}_{70}\text{Te}_{30}$  AMLs as photogenerating layers, display high photosensitivity over the entire visible and near infrared regions.

## 2. Effect of Te content

Room temperature Raman spectra of  $\text{Se/Se}_{100-x}\text{Te}_x$  AMLs having fixed thicknesses of  $4$  and  $7\text{ nm}$  for  $\text{Se}$  and  $\text{Se}_{100-x}\text{Te}_x$  sublayers, respectively, are shown in Figs. 2(a)–2(c) for three different  $\text{Te}$  contents and various laser power densities. Each spectrum corresponds to different spot of the respective sample, but to the same exposure time of  $30\text{ min}$  (recording time). The laser power density was gradually increased from  $17$  to  $50\text{ W/cm}^2$ . As the optical band gap of  $\text{Se}_{100-x}\text{Te}_x$  alloys increases with decreasing  $\text{Te}$  content, the  $530.9\text{ nm}$   $\text{Kr}^+$  laser line has been used in this series of experiments in order to ensure a comparable light absorption in the  $\text{Se}_{100-x}\text{Te}_x$  sublayers of all  $\text{Se/Se}_{100-x}\text{Te}_x$  AMLs ( $\alpha > 10^5\text{ cm}^{-1}$  for the three  $\text{Te}$  contents<sup>11</sup> used in these experiments).

It is obvious from Fig. 2 that crystallization in  $\text{Se/Se}_{70}\text{Te}_{30}$  AMLs is very weak (nearly absent) when the sample is illuminated by a power density of  $17\text{ W/cm}^2$ , but it becomes stronger as the power density is increased [Fig. 2(c)]; also, in the AML with this  $\text{Te}$  content, we observe no peak at  $252\text{ cm}^{-1}$  for the highest power density used, which implies total crystallization in both  $\text{Se}$  and  $\text{Se}_{70}\text{Te}_{30}$  sublayers. On the contrary, the presence of the  $252\text{ cm}^{-1}$  of  $a\text{-Se}$  in all  $\text{Se/Se}_{100-x}\text{Te}_x$  AMLs with  $x = 7.5$  and  $15$  implies that crystallization is not as efficient as in AMLs with  $x = 30$ . These observations indicate that the thermal stability of AMLs decreases with increasing  $\text{Te}$  content. In order to verify whether this is valid for three-dimensional samples of  $\text{Se}_{100-x}\text{Te}_x$ , we have studied Raman scattering from  $\text{Se}_{100-x}\text{Te}_x$  single layers ( $x = 0, 7.5, 15$ , and  $30$ ) having a thickness of  $2\text{ }\mu\text{m}$ . These spectra (Fig. 3) were excited by the  $530.9\text{ nm}$   $\text{Kr}^+$  laser line at a power density of  $50\text{ W/cm}^2$  and correspond to an exposure time equal to the recording time ( $30\text{ min}$ ). Taking the intensity of the  $235\text{ cm}^{-1}$  band as a measure of crystallization, one can infer that crystallization in the  $\text{Se}_{70}\text{Te}_{30}$  layer is almost absent, but its extent increases with decreasing  $\text{Te}$  content, becoming strongest in the pure  $\text{Se}$  layer. Hence, the observed compositional dependence of

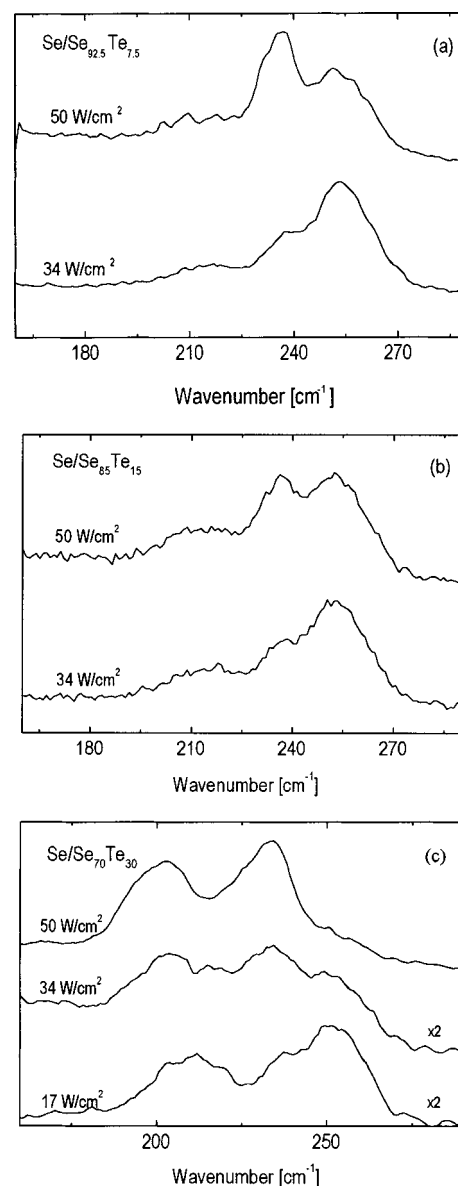


FIG. 2. Room temperature Raman spectra of  $\text{Se/Se}_{100-x}\text{Te}_x$  AMLs having fixed  $\text{Se}$  and  $\text{Se}_{100-x}\text{Te}_x$  sublayer thicknesses of  $4$  and  $7\text{ nm}$ , respectively, and with  $x$  values ( $\text{Te}$  contents) of (a)  $7.5$ , (b)  $15$ , and (c)  $30$  excited by various power densities of the  $530.9\text{ nm}$   $\text{Kr}^+$  laser line. Each spectrum corresponds to different spot of the respective sample, but to the same exposure time ( $30\text{ min}$ ) which corresponds to the recording time of the spectra.

the structural stability of  $\text{Se}_{100-x}\text{Te}_x$  single layers exposed by intense laser light is in contradiction with that obtained for  $\text{Se/Se}_{100-x}\text{Te}_x$  AMLs.

In order to address the above contradictory results, we recall the thermodynamic approach of Tanaka *et al.*,<sup>19</sup> who consider an amorphous layer  $A$  having a thickness smaller than the critical embryo radius  $r_c$  being sandwiched between two layers of a high-refractivity amorphous material  $B$ . It has been shown that  $T_c$  should increase with decreasing sublayer thickness  $d_A$  if the interfacial free energy  $E_{aa}$  between  $A$  and both  $B$  amorphous sublayers is higher than the corresponding energy  $E_{ac}$  between amorphous and crystalline sublayers. In the opposite case (i.e.,  $E_{aa} < E_{ac}$ ),  $T_c$  must decrease with decreasing  $d_A$ . In our previous study of  $\text{Se/CdSe}$  AMLs,<sup>10</sup>

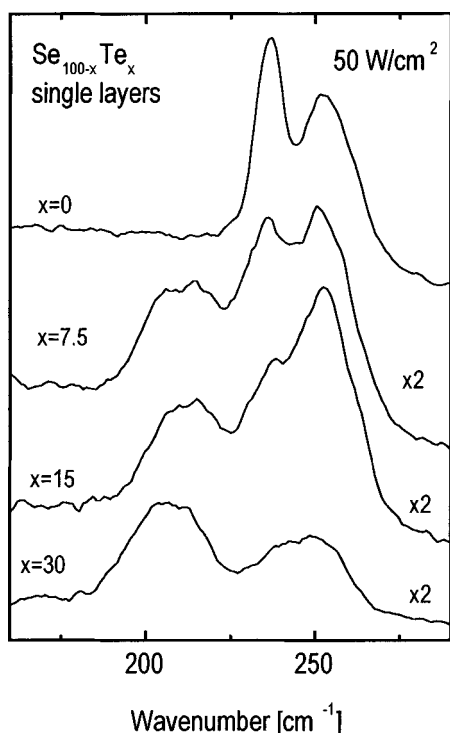


FIG. 3. Room temperature Raman spectra of  $\text{Se}_{100-x}\text{Te}_x$  single layers of fixed thickness ( $2\ \mu\text{m}$ ) and various compositions ( $x=0, 7.5, 15, 30$ ) excited by various power densities of the  $530.9\ \text{nm}$   $\text{Kr}^+$  laser line.

we have reported an increase of crystallization temperature of Se with decreasing sublayer thickness. A comparison of the spectra of Fig. 2 with those of  $\text{Se}/\text{CdSe}$  AMLs<sup>10</sup> indicates that the extent of crystallization in Se sublayers of both  $\text{Se}$  ( $3.5\ \text{nm}$ )/ $\text{CdSe}$  and  $\text{Se}$  ( $4\ \text{nm}$ )/ $\text{Se}_{100-x}\text{Te}_x$  ( $x=7.5$  and  $15$ ) AMLs is similar (i.e., the integrated intensities of the  $235$  and  $252\ \text{cm}^{-1}$  are almost equal) when they are exposed to strongly absorbed light ( $488$  and  $530.9\ \text{nm}$ , respectively) at a power density of  $50\ \text{W}/\text{cm}^2$ . However, under the same exposure, crystallization in  $\text{Se}$  ( $4\ \text{nm}$ )/ $\text{Se}_{70}\text{Te}_{30}$  AMLs is much stronger, but it remains weaker than that in  $\text{Se}$  single layers having thickness of about  $200\ \text{nm}$ .<sup>10</sup> These results may be explained if one assumes that  $T_c$  of Se sublayers in all AMLs is higher than that of bulk Se, with the magnitude of this increase depending largely on the nature of material B. It seems that in  $\text{Se}/\text{Se}_{100-x}\text{Te}_x$  AMLs, the higher the Te content, the smaller the  $T_c$  increase in Se sublayers.

### B. Stability under illumination

In order to study photoinduced structural changes in  $\text{Se}/\text{Se}_{100-x}\text{Te}_x$  AMLs free of thermally induced effects during the measurements, Raman scattering spectra of these AMLs were recorded at  $38\ \text{K}$ , using the strongly absorbed  $530.9\ \text{nm}$   $\text{Kr}^+$  laser line. There has not been to date a study concerning the compositional dependence of pure photoinduced crystallization in two-dimensional layers of  $\text{Se}_{100-x}\text{Te}_x$  alloys. As the structural changes observed at low temperatures are weaker, we have also used in this series of measurements longer exposure times (than the  $30\ \text{min}$  corresponding to the recording time) by illuminating the sample

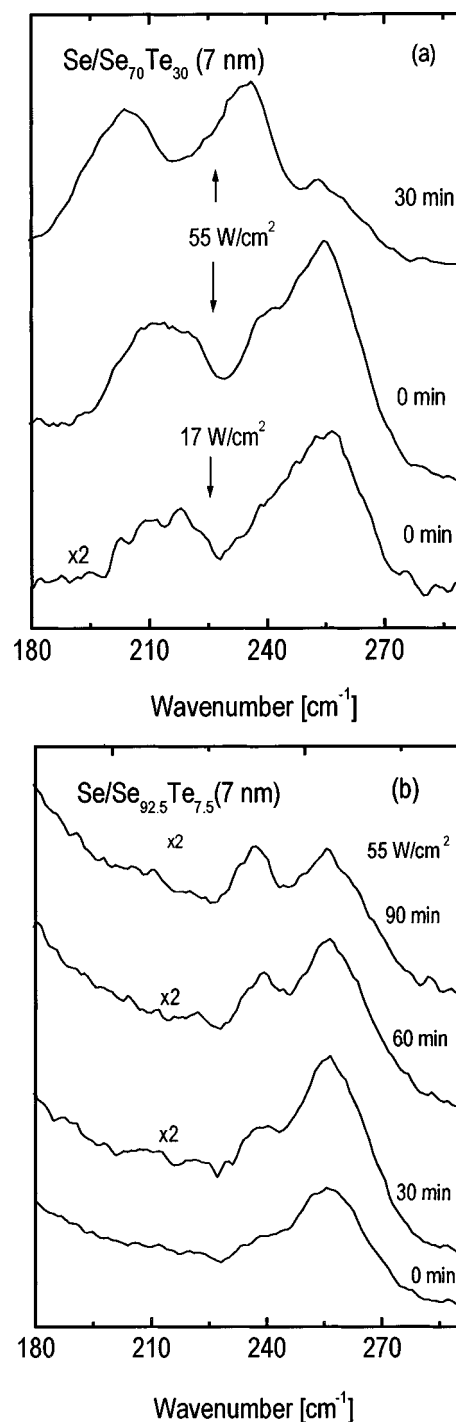


FIG. 4. Low temperature ( $38\ \text{K}$ ) Raman spectra of  $\text{Se}/\text{Se}_{100-x}\text{Te}_x$  AMLs having fixed Se and  $\text{Se}_{100-x}\text{Te}_x$  sublayer thicknesses of  $4$  and  $7\ \text{nm}$ , respectively and with  $x$  values (Te contents) of (a)  $30$  and (b)  $7.5$ , excited by power densities of (a)  $17$  and  $55\ \text{W}/\text{cm}^2$ , and (b)  $55\ \text{W}/\text{cm}^2$  of the  $530.9\ \text{nm}$   $\text{Kr}^+$  laser lines, and for various preliminary exposure times. Each spectrum corresponds to different spot of the respective sample.

(at  $38\ \text{K}$ ) with the same laser beam prior to the spectrum recording. The Raman spectra of two  $\text{Se}/\text{Se}_{100-x}\text{Te}_x$  AMLs with  $x=30$  and  $7.5$  at  $38\ \text{K}$  are shown in Figs. 4(a) and 4(b), respectively. It can be seen from Fig. 4(a) that the  $235\ \text{cm}^{-1}$  band is almost absent for the lower power density of  $17\ \text{W}/\text{cm}^2$  (i.e., there is no substantial photoinduced crystallization in the  $\text{Se}/\text{Se}_{70}\text{Te}_{30}$  AML), is marginally observed at a

power density of 55 W/cm<sup>2</sup> (without previous exposure) and becomes well pronounced when the spectrum is recorded after a preliminary exposure at the same intensity for 30 min. In Se/Se<sub>92.5</sub>Te<sub>7.5</sub> AML [Fig. 4(b)], using similar experimental conditions, photoinduced crystallization is less efficient even after longer preliminary exposures to the same power density. This result indicates that the higher the Te content, the higher the extent of photoinduced crystallization in Se/Se<sub>100-x</sub>Te<sub>x</sub> AMLs.

In the first works on photocrystallization of *a*-Se, it has been found<sup>22,23</sup> that exposure to light enhances thermal crystallization. Further studies carried out at low temperatures<sup>14,15</sup> ( $T=77$  and 100 K, respectively) have shown that in *a*-Se thin films, pure photocrystallization takes place above a “threshold” power of about 250 W/cm.<sup>14</sup> Systematic investigations on glassy samples and thin films of Se<sub>100-x</sub>Te<sub>x</sub> have shown<sup>24-26</sup> that photocrystallization is highly dependent on the alloy composition. It has been found that the rate of crystallization is almost zero for  $x=4-5$ ,<sup>24,26</sup> it increases sharply for  $x$  up to 10 and then slowly for  $x$  up to 30.<sup>25,26</sup> In the Se/Se<sub>100-x</sub>Te<sub>x</sub> AMLs studied here, well-expressed photocrystallization is seen for an exposure at 55 W/cm<sup>2</sup> [Fig. 4(a)] which is much lower than the “threshold” power of 250 W/cm<sup>2</sup> for *a*-Se.<sup>14</sup> That is why we consider that changes observed in the Raman spectra of the present AMLs may be related to photocrystallization in Se<sub>100-x</sub>Te<sub>x</sub> sublayers. Hence, we conclude that in two-dimensional Se<sub>100-x</sub>Te<sub>x</sub> layers, the compositional dependence of the strength of photocrystallization is similar to that reported in three-dimensional samples.<sup>24-26</sup>

As was mentioned in the previous chapter, the increase of Te content leads to a gradual increase of thermal crystallization temperature and thus to an improvement of thermal stability of Se<sub>100-x</sub>Te<sub>x</sub> alloys.<sup>1,27</sup> On the other hand, the rate of photocrystallization increases with increasing Te content.<sup>24-26</sup> These opposite effects of Te on thermal and light stability of *a*-Se might be understood in terms of different mechanisms responsible for each crystallization process. It has been reported<sup>27</sup> that viscosity is the key quantity in the case of thermal crystallization. The  $T_c$  increase has been ascribed to an increase of the average molar mass by the inclusion of heavier tellurium atoms in the Se chains, resulting in a viscosity increase with  $x$ . The microscopic mechanism of photocrystallization is still a matter of discussion, but it is considered<sup>18,22,28</sup> that amorphous-to-crystalline structural changes are enhanced by photoexcited carriers which cause the breaking of covalent bonds followed by the creation of new bonds at other network positions. Should this be the case, the bond energy becomes important in this process and bearing in mind the difference in Se–Se (1.9 eV) and Se–Te (~1.8 eV) bond energies,<sup>27</sup> one may anticipate the observed increase of the photocrystallization strength with increasing Te content in both three-dimensional Se<sub>100-x</sub>Te<sub>x</sub> and two-dimensional Se<sub>100-x</sub>Te<sub>x</sub> sublayers having equal thicknesses.

#### IV. CONCLUSIONS

Compositional and thickness dependent changes of the structural stability of amorphous Se/Se<sub>100-x</sub>Te<sub>x</sub> multilayers

( $x=7.5$ , 15, and 30) have been studied under thermal and light treatments. These treatments have been applied using the 647.1 and 530.9 nm Kr<sup>+</sup> laser lines at a power density varying between 17 and 135 W/cm<sup>2</sup>. The sublayer thickness dependence of thermal stability of the AMLs has been investigated at room temperature in the case of Se/S<sub>70</sub>Te<sub>30</sub> AMLs using the red laser line (which is strongly absorbed by the Se<sub>70</sub>Te<sub>30</sub> sublayers, but weakly so by the Se ones). On the other hand, the Te-content dependence of the thermal stability has been studied using the green line. It has been observed that: (i) the crystallization temperature of Se<sub>70</sub>Te<sub>30</sub> sublayers (and therefore the AML stability) increases with decreasing their sublayer thickness, while (ii) the crystallization temperature of Se sublayers (having a fixed thickness of 4.0 nm) depends on the Te content of the Se<sub>100-x</sub>Te<sub>x</sub> sublayer, i.e., it is higher, the lower the Te content. The first result is in accordance with those reported previously for *a*-Ge:H,<sup>19,20</sup> and *a*-Se.<sup>10,21</sup> As for the second result, it may be expected from thermodynamic considerations,<sup>19</sup> but it is observed for the first time in Se/Se<sub>100-x</sub>Te<sub>x</sub> AMLs.

The photoinduced structural changes in Se/Se<sub>100-x</sub>Te<sub>x</sub> AMLs have been explored at a low temperature (38 K) for which thermally induced photocrystallization is not anticipated. It has been found that exposure to the green laser line leads to photoinduced crystallization, the rate of which increases with increasing Te content, a result which is in agreement with previous reports on three-dimensional Se<sub>100-x</sub>Te<sub>x</sub> alloys,<sup>24-26</sup> implying that there should not be a considerable change in Se–Se and Se–Te bond energies when a dimensionality reduction (from 3 to 2) takes place in the alloys.

#### ACKNOWLEDGMENTS

One of the authors (D.N.) wishes to thank NATO and the Finance Ministry of Greece for supporting a scientific visit to the Physics Department of the National Technical University of Athens where Raman scattering measurements were carried out. D.N. and D.A. are also grateful to the Bulgarian Ministry of Education and Science for financial support for the preparation of samples for this project (Contract F-505).

<sup>1</sup>S. O. Kasap, in *Handbook of Imaging Materials*, edited by A. S. Diamond (Marcel Dekker, New York, 1991), p. 355.

<sup>2</sup>E. Maruyama, Jpn. J. Appl. Phys., Part 1 **21**, 231 (1982).

<sup>3</sup>M. Abkowitz, in *Physics of Disordered Materials*, edited by D. Alder, H. Fritzschke, and S. R. Ovshinski (Plenum, New York, 1984), p. 483.

<sup>4</sup>S. O. Kasap, M. Ba Xendale, and C. Juhász, IEEE Trans. Ind. Appl. **27**, 620 (1991).

<sup>5</sup>D. Arsova, D. Nesheva, and E. Vateva, in *Proceedings of the 8th ISCMP, Varna '94*, edited by J. Marshall, N. Kirov, and A. Vavrek (Research Studies Press Ltd., 1995), p. 299.

<sup>6</sup>D. Nesheva, D. Arsova, and E. Vateva, Semicond. Sci. Technol. **12**, 595 (1997).

<sup>7</sup>E. Vateva and I. Georgieva, J. Non-Cryst. Solids **164–165**, 865 (1993).

<sup>8</sup>E. Vateva and I. Georgieva, J. Non-Cryst. Solids **114**, 124 (1989).

<sup>9</sup>R. Ionov and D. Nesheva, Thin Solid Films **213**, 230 (1992).

<sup>10</sup>D. Nesheva, I. P. Kotsalas, C. Raptis, and E. Vateva, J. Non-Cryst. Solids **224**, 283 (1998).

<sup>11</sup>H. Adachi and K. C. Kao, J. Appl. Phys. **51**, 6326 (1980).

<sup>12</sup>D. Nesheva, D. Arsova, and Z. Levi, Philos. Mag. **70**, 205 (1994).

<sup>13</sup>A. Mooradian and G. B. Wright, in *Physics of Selenium and Tellurium*, edited by W. C. Cooper (Pergamon, Oxford, 1969), p. 269.

- <sup>14</sup>A. A. Baganich, V. I. Mikla, D. G. Semak, A. P. Sokolov, and A. P. Shebanin, *Phys. Status Solidi B* **166**, 247 (1991).
- <sup>15</sup>P. Nagels, E. Sleetckx, R. Callaerts, and L. Tichy, *Solid State Commun.* **94**, 49 (1995).
- <sup>16</sup>H. P. Grunwald, *Mater. Res. Bull.* **7**, 543 (1972).
- <sup>17</sup>R. M. Martin, G. Lucovsky, and K. Helliwell, *Phys. Rev. B* **13**, 1383 (1976).
- <sup>18</sup>A. Roy, A. V. Kolobov, and K. Tanaka, *J. Appl. Phys.* **83**, 4951 (1998).
- <sup>19</sup>K. Tanaka, I. Honma, H. Tamaoki, and H. Komiyama, *Mater. Res. Soc. Symp. Proc.* **118**, 343 (1988).
- <sup>20</sup>H. Xu, Y. Wang and G. Chen, *Phys. Status Solidi A* **143**, K87 (1994).
- <sup>21</sup>A. Kikineshy, *Opt. Eng. (Bellingham)* **34**, 1040 (1995).
- <sup>22</sup>J. Dresner and B. B. Stringfellow, *J. Phys. Chem. Solids* **29**, 303 (1968).
- <sup>23</sup>K. S. Kim and D. Turnbull, *J. Appl. Phys.* **45**, 3447 (1974).
- <sup>24</sup>M. Okuda, T. Matsushita, and A. Suzuki, *Proceedings Symposium of Physics of Se and Te* (Koningstein, Germany, 1979), p. 270.
- <sup>25</sup>R. Misra, S. K. Tripathi, A. K. Agnihotri, and A. Kumar, *Solid State Commun.* **77**, 797 (1991).
- <sup>26</sup>S. K. Srivastava, A. K. Agnihotri, A. Kumar, S. Swarup, and A. N. Nigama, *Jpn. J. Appl. Phys., Part 2* **32**, L557 (1993).
- <sup>27</sup>S. O. Kasap and C. Juhasz, *J. Mater. Sci.* **21**, 1329 (1986).
- <sup>28</sup>A. V. Kolobov, V. Lyubin, T. Yasuda, and K. Tanaka, *Phys. Rev. B* **55**, 23 (1997).